

<https://doi.org/10.1038/s43247-024-01765-1>

Freeze-thaw strength increases microbial stability to enhance diversity-soil multifunctionality relationship

Check for updates

Shengyun Chen^{1,2,7}✉, Yuzheng Gu^{1,3,7}, Enyan Liu², Minghui Wu^{1,4}, Xiaoli Cheng⁴, Peizhi Yang³, Ali Bahadur¹, Ruiqiang Bai¹, Jianwei Chen⁵, Mingyi Zhang¹, Jihua Wu²✉ & Qi Feng⁶

Insights into the impacts of freeze-thaw processes on soil microorganisms and their related functions in permafrost regions are crucial for assessing ecological consequences imposed by the shifts in freeze-thaw patterns. Through in-situ investigations on seasonal freeze-thaw processes in the active layer of permafrost in the Qinghai-Tibet Plateau, we found that microbial richness was higher and positively correlated with soil multifunctionality during the freeze-thaw stage (freezing and thawing periods) compared to the non-freeze-thaw stage (completely frozen and thawed periods). This relationship resulted from the higher microbial stability, which was highly consistent with the lower complexity, more keystone taxa, and greater robustness of networks. Although freeze-thaw strength exacerbated the greenhouse effect on climate, it was alleviated by the enhancement of diversity-soil multifunctionality relationship. These findings have substantial implications for exploring the responses of microbial-mediated soil multifunctionality and greenhouse effect in alpine permafrost to more drastic variations of freeze-thaw processes under future warming.

As a sensitive indicator of climate change, freeze-thaw processes are caused by diurnally or seasonal thermal changes following water phase transition in the topsoil to a certain depth¹. The processes are exceedingly frequent in the active layer surface of high-altitude (alpine) and high-latitude permafrost^{2,3}. Over the past several decades, observational studies have shown that freeze-thaw patterns have varied drastically⁴, as evidenced by the increases in the freeze-thaw and completely thawed days, but a decrease in the completely frozen days⁵, as well as an ulterior increase in maximum thawing depth⁶. Based on experimental warming and model simulation, freeze-thaw strength, reflecting the magnitude and frequency of changes in soil temperature above and below 0 °C^{7,8}, is expected to increase further, with extended durations of the freeze-thaw stage including the thawing and freezing periods in the future^{1,9}. Laboratory simulations and meta-analysis have demonstrated that the changes in freeze-thaw processes alter soil structure such as porosity and aggregates^{10,11}, exerting strong influences on microbial composition and diversity^{12,13}. Meanwhile, a few studies have shown that freeze-thaw processes can cause large shifts in the structure of

microbial communities^{14–16}, including increased bacterial diversity when the soil is completely thawed compared to frozen soil. These microbial shifts in turn play a critical role in soil functions, such as nutrient provisioning^{13,17}, element cycling¹⁸, and gas emission¹⁹. Despite this knowledge, there is still a scarcity of in-situ observations on the effects of freeze-thaw processes, especially seasonal freeze-thaw processes, on microbial structure and stability, which can serve as an important foundation for assessing the impact of shifted freeze-thaw patterns on the microbial-mediated soil functions.

Soil functions are multivariate²⁰, allowing the use of an integrative measure of multiple soil functions, known as multifunctionality, to quantify and compare the capability of soil ecosystems to fulfill various ecological roles^{21,22}. Numerous studies have shown that diversities of various types of soil organisms, such as microorganisms, can drive or inhibit soil multifunctionality^{21,23–25}. Therefore, the relationships between microbial diversity and soil multifunctionality have become a central and controversial topic in microbial ecology²⁶. A previous study under simulated freeze-thaw conditions revealed that soil multifunctionality

¹Cryosphere and Eco-Environment Research Station of Shule River Headwaters, Key Laboratory of Cryospheric Science and Frozen Soil Engineering, Northwest Institute of Eco-Environment and Resources, Chinese Academy of Sciences, Lanzhou, Gansu, China. ²State Key Laboratory of Herbage Improvement and Grassland Agro-ecosystems, College of Ecology, Lanzhou University, Lanzhou, Gansu, China. ³College of Grassland Agriculture, Northwest A&F University, Yangling, Shaanxi, China. ⁴Key Laboratory of Soil Ecology and Health in Universities of Yunnan Province, School of Ecology and Environmental Sciences, Yunnan University, Kunming, Yunnan, China. ⁵BGI-Qingdao, BGI-Shenzhen, Qingdao, Shandong, China. ⁶Key Laboratory of Ecohydrology of Inland River Basin/Gansu Qilian Mountains Eco-Environment Research Center, Northwest Institute of Eco-Environment and Resources, Chinese Academy of Sciences, Lanzhou, Gansu, China. ⁷These authors contributed equally: Shengyun Chen, Yuzheng Gu. ✉e-mail: syichen@zb.ac.cn; wjh@lzu.edu.cn

was largely governed by fungal diversity rather than bacterial diversity¹³. Importantly, the unique physiological characteristics of bacteria and fungi can result in metabolic labor division, leading to microbial communities complementary²⁴. Hence, it is essential to comprehensively investigate the periodic changes in the relationship between microbial diversity and soil multifunctionality during the freeze-thaw processes, which can help identify the potential ecological consequences.

A growing body of research has focused on exploring the linkages between microbial co-occurrence networks and soil multifunctionality^{21,24,27}, with network complexity or keystone taxa playing an important role in influencing multifunctionality^{22,26,28}. Indeed, microbial networks with lower complexity as characterized by multiple network properties (e.g., degree and centrality), fewer keystone taxa identified through within- and among-module connectivity, and greater robustness measured by natural connectivity after removing edges, can reflect greater stability of microbial communities^{22,29–31}. Consequently, more stable communities can better maintain soil multifunctionality in the face of environmental disturbances³². According to a recent study, microbial stability may determine the direction and strength of the microbial diversity-soil multifunctionality relationship²⁴. Hence, it is necessary to explore how microbial stability responds to seasonal freeze-thaw processes and participates in regulating the diversity-soil multifunctionality relationship, which can be a key to understand the mechanisms underpinning this complex relationship.

However, the preceding efforts were primarily undertaken in laboratory simulations, which cannot accurately reflect the in-situ processes under natural conditions. Especially, field investigations are absolutely scarce in permafrost regions of the Qinghai-Tibet Plateau (QTP), where sampling is challenging in spring and winter¹⁴, yet it is a hotspot for frequent freeze-thaw processes due to the broad daily and annual temperature ranges^{5,33}. Thus, to comprehensively investigate the effects of freeze-thaw processes on microbial communities and soil multifunctionality in natural conditions, we incorporated in-situ observations during the thawing, freezing, completely thawed, and completely frozen periods at 0–10 cm and 10–20 cm depths in the active layer of alpine permafrost, in the Shule River headwaters of the northeast margin of the QTP, China. We examined microbial communities using high-throughput sequencing and obtained a data set of 17 soil functions to assess multifunctionality, including nutrient provisioning, element cycling, and gas emission. We also combined the thawing and freezing periods into the freeze-thaw stage and the completely thawed and frozen periods into the non-freeze-thaw stage to assess the related impacts caused by variations in the freeze-thaw strength. We aimed to test three main hypotheses: (i) Microbial communities can maintain higher diversity and stability during the freeze-thaw stage compared to the non-freeze-thaw stage; (ii) Microbial diversity can support soil multifunctionality and their relationship depending on microbial stability; and (iii) Increasing freeze-thaw strength can exacerbate the greenhouse effect.

Results

Composition and diversity of microbial community

The dominant phyla in microbial communities were consistent among four periods and between two depths (Supplementary Table S1). Specifically, the dominant bacterial phyla were *Bacteroidetes* (30%), *Proteobacteria* (22%), *Acidobacteria* (15%), and *Actinobacteria* (10%), while the dominant fungal phyla were *Ascomycota* (72%) and *Zygomycota* (14%). The relative abundances of *Actinobacteria*, *Chloroflexi*, *Gemmatimonadetes*, *Verrucomicrobia*, *Basidiomycota*, and *Chytridiomycota* varied significantly among periods. In addition, *Verrucomicrobia* and *Basidiomycota* had the greater relative abundances during the non-freeze-thaw stage than the freeze-thaw stage, and the relative abundance of *Proteobacteria* was obviously greater in 0–10 cm than 10–20 cm layer (Supplementary Table S1). Bacterial richness was significantly higher during the freeze-thaw stage than the non-freeze-thaw stage, while fungal richness reached the highest in the freezing period and the lowest in the completely thawed period, and microbial richness also showed the same trend (Supplementary Fig. S3). Furthermore, bacterial, fungal, and microbial richness were all significantly higher in 0–10 cm than

10–20 cm layer (Supplementary Fig. S3). The random forest model revealed that freeze-thaw strength and maximum thawing depth were the important variables affecting microbial diversity (Supplementary Fig. S4).

Microbial co-occurrence network and stability

Microbial co-occurrence networks were constructed to evaluate possible ecological interactions among bacterial and fungal communities across the seasonal freeze-thaw processes and soil profile (Fig. 1A). We found more bacterial and fungal nodes, and fungi-fungi links, but fewer bacteria-bacteria and bacteria-fungi links during the freeze-thaw stage than the non-freeze-thaw stage (Supplementary Fig. S5). Networks of the non-freeze-thaw stage also had higher density and transitivity, but lower average path length and modularity. Degree, linkage density, and closeness centrality were significantly lower, but betweenness centrality was higher during the freeze-thaw stage (Fig. 1B). Consequently, the network complexity calculated by these properties (Supplementary Fig. S6) was significantly lowest in the thawing period and highest in the completely frozen period, as well as higher during the non-freeze-thaw stage than the freeze-thaw stage (Supplementary Fig. S5A). In terms of depth, 0–10 cm layer had lower density and transitivity, but higher modularity, while 10–20 cm layer had significantly higher degree, linkage density, and closeness centrality, but lower betweenness centrality (Fig. 1B). In addition, more keystone taxa were identified during the freeze-thaw stage and in 0–10 cm layer (Supplementary Fig. S7). Meanwhile, natural connectivity of networks decreased significantly to a greater extent during the freeze-thaw stage than the non-freeze-thaw stage and in 10–20 cm than 0–10 cm layer by removing the same proportion of edges, indicating the weaker robustness (Fig. 1C and Supplementary Table S2). These results showed that microbial communities exhibited more stable network structures during the freeze-thaw stage and in 0–10 cm layer^{31,34}. We also used the method of the average variation degree to directly assess microbial stability and obtained the consistent results that the freeze-thaw stage exhibited higher microbial stability (Fig. 1D). Furthermore, the random forest model showed that bacterial node, soil temperature, and bacteria-fungi links were important in predicting microbial stability (Supplementary Fig. S8). Especially, bacterial nodes were positively, but bacteria-fungi links was negatively associated with microbial stability. Network complexity was also proved to show a negative association with microbial stability (Supplementary Fig. S9).

Soil multifunctionality

A total of 17 soil parameters were measured as individual soil functions and categorized into three groups of multifunctionality based on their connections to related functions (i.e., Ca^{2+} , K^+ , NH_4^+ , etc. were pooled into the element cycling category; see *Statistical Analysis* for details). We found that there were significant differences in soil water-soluble organic carbon (WSOC), microbial biomass carbon (MBC), $\text{NH}_4^+\text{-N}$, NO_3^- , SO_4^{2-} , Ca^{2+} , K^+ , methane (CH_4) flux, and nitrous oxide (N_2O) flux among periods. Notably, CH_4 was emitted solely in the completely frozen period and absorbed in the other periods. Organic carbon (OC), MBC, total nitrogen (TN), $\text{NO}_3^-\text{-N}$, microbial biomass nitrogen (MBN), NO_2^- , and carbon dioxide (CO_2) flux were obviously higher in 0–10 cm layer than 10–20 cm layer (Supplementary Fig. S10A–C). In terms of the classified soil multifunctionality, multielement was significantly lowest in the completely thawed period, and multinutrient was significantly greater in 0–10 cm than 10–20 cm layer. For soil multifunctionality and global warming potential (GWP), they were both obviously greater in 0–10 cm than 10–20 cm layer (Supplementary Figs. S10D and S11).

In general, soil water content, microbial diversity, and freeze-thaw strength were the considerable variables impacting soil multifunctionality tested by random forest model (Supplementary Fig. S13). We focused on identifying what affected multigas and its individual functions. Multinutrient and freeze-thaw strength positively contributed the most to CO_2 and N_2O fluxes, respectively, while soil temperature exhibited the greatest negative contribution to CH_4 flux. Soil porosity (Por) and freeze-thaw strength were the essential drivers with positive effects on multigas

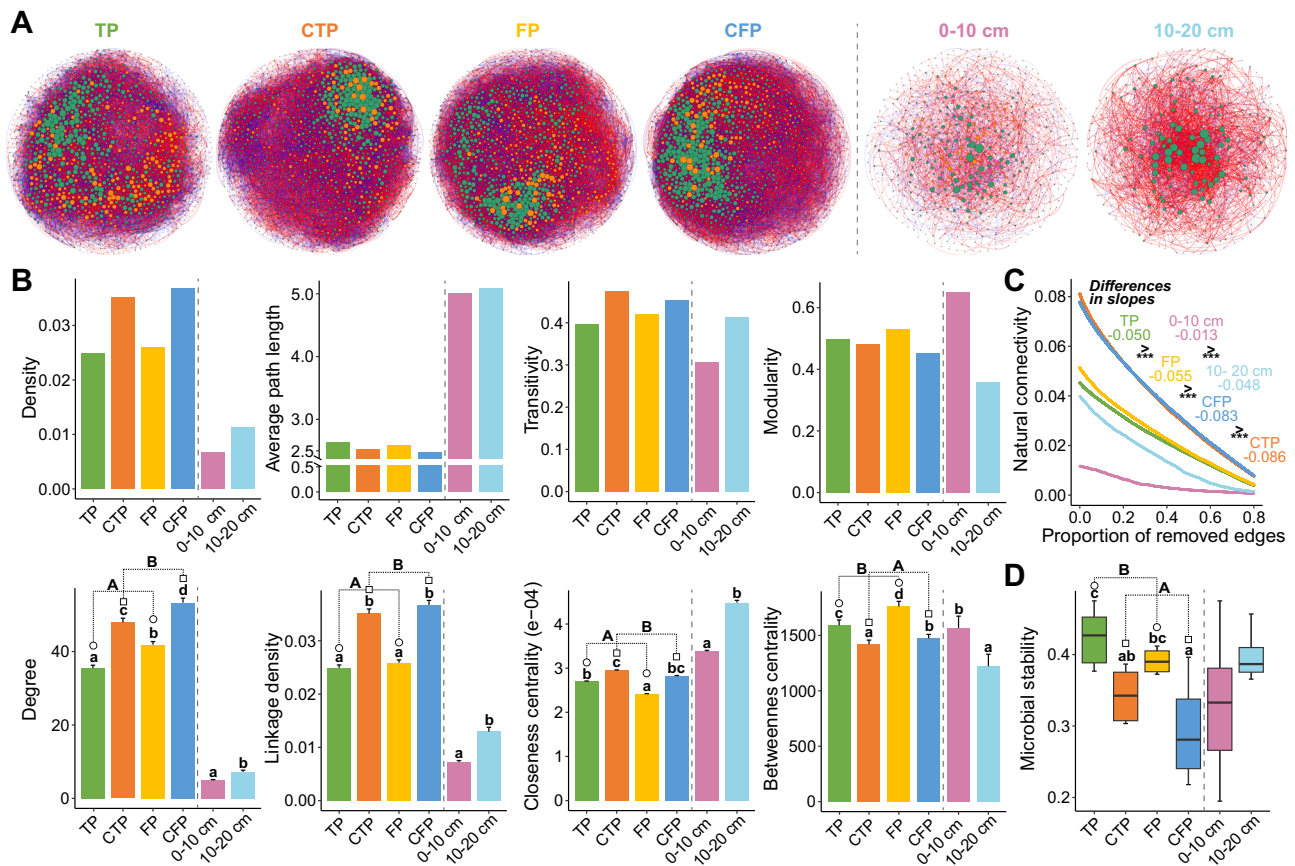


Fig. 1 | Co-occurrence networks and stability of microbial community during four periods of seasonal freeze-thaw processes and at two depths. **A** In microbial networks, nodes represent individual operational taxonomic units (OTUs), green nodes are bacteria and orange nodes are fungi, whose size are positively correlated with the node degree; edges represent significant correlations ($R > 0.8$ and $p < 0.05$), which red lines indicate positive correlations and blue lines indicate negative correlations. **B** Differences of multiple network properties, including density, average path length, transitivity, modularity, degree, linkage density, closeness centrality, and betweenness centrality among four periods and between two depths (mean \pm se). **C** Robustness analysis is shown as the relationship between microbial natural

connectivity and the proportion of removed edges, with larger variations of natural connectivity upon the same proportions indicating less robustness or stability of microbial networks. **D** Differences of the stability of microbial communities among four periods and between two depths (mean \pm se). TP, CTP, FP, and CFP represent the thawing, completely thawed, freezing, and completely frozen periods, respectively. Lowercase letters represent the significance of differences among four periods or between two depths, and uppercase letters represent the significance of differences between the freeze-thaw and non-freeze-thaw stages. Asterisks indicate the statistical significance (** $p < 0.001$, ** $p < 0.01$, and * $p < 0.05$).

(Supplementary Fig. S13). Furthermore, structural equation model (SEM) revealed that 64.5% of the variance in CO₂ flux was explained, which was mainly affected positively by multinutrient. The variance in CH₄ flux was interpreted by 42.6%, with maximum thawing depth and freeze-thaw strength having large negative effects. Freeze-thaw strength was primarily responsible for N₂O flux, with 38.7% of the variance being explained (Fig. 2A, B).

Relationships among microbial diversity, stability, and soil multifunctionality

We further explored the relationships among microbial diversity, stability, and soil multifunctionality. No significant link was observed between microbial diversity and stability, but microbial diversity was positively correlated with soil multifunctionality (Supplementary Fig. S14A and B). In particular, this relationship between microbial diversity and soil multifunctionality occurred only during the freeze-thaw stage (Fig. 3A). When considering soil individual functions and classified soil multifunctionalities, microbial diversity had more positive correlations with them during the freeze-thaw stage and in 0–10 cm layer (Fig. 3B). Moreover, we found that the proportions of microbial taxa supporting multinutrient, multielement, and multigas were all lower during the non-freeze-thaw stage and in 10–20 cm layer (Fig. 3C).

There was no significant association of microbial stability with soil multifunctionality (Supplementary Fig. S14C). Interestingly, we found that the stability of microbial communities was positively relevant with the diversity-multifunctionality relationship (Fig. 4A). The random forest model showed that microbial stability, belowground biomass (BGB), and freeze-thaw strength were crucial in predicting this relationship (Supplementary Fig. S15). The SEM suggested that the variance in microbial diversity-soil multifunctionality relationship was explained by 40.9%, and the positive effect of microbial stability on this relationship was retentive, and largest when considering simultaneously environmental variables including freeze-thaw strength, maximum thawing depth, and soil properties. Moreover, microbial stability was regulated by freeze-thaw strength, which also had a strongly positive effect on this relationship. Notably, 61.8% of the variance in GWP was explained, which was negatively influenced by microbial diversity-soil multifunctionality relationship, as well as significantly driven by freeze-thaw strength (Fig. 4B, C).

Discussion

Our findings proved that microbial richness was higher during the freeze-thaw stage and in 0–10 cm layer, most likely due to several reasons. Firstly, greater freeze-thaw strength may facilitate the disruption of aggregate structures and release nutrients^{35,36}, allowing for more abundant and diverse

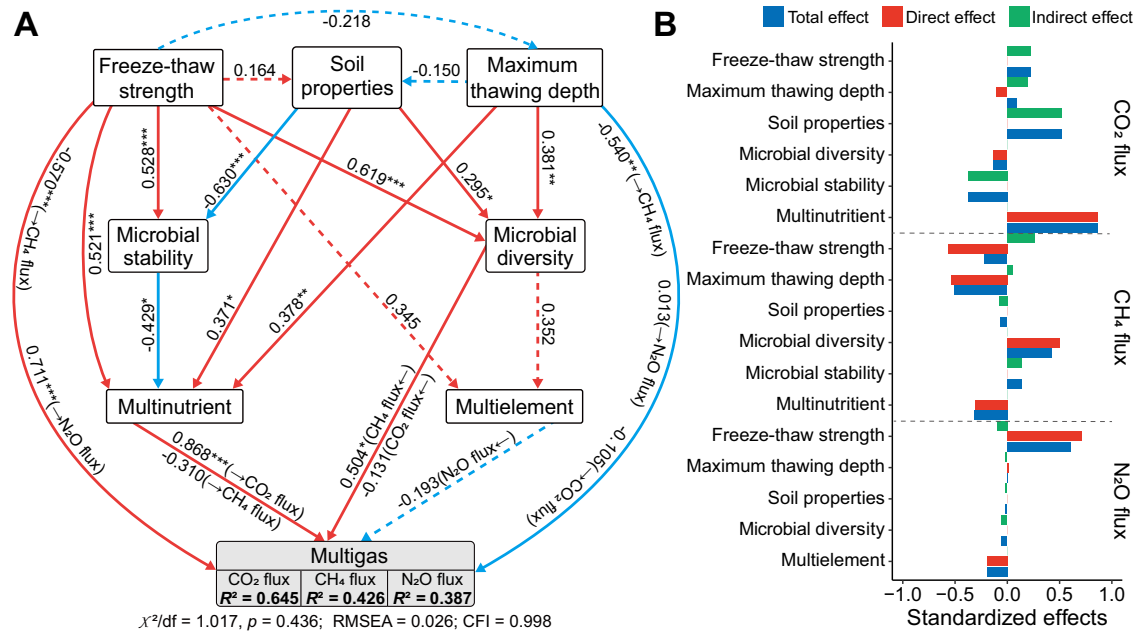


Fig. 2 | Variables affecting soil gas fluxes. **A** Structural equation model (SEM) describing the effects of freeze-thaw strength, maximum thawing depth, soil properties, microbial diversity, stability, multielement, and multinutrient on multigas (CO₂, CH₄, and N₂O fluxes). Three fluxes were grouped into one box in the model for graphical simplicity; however, the box does not represent latent variables. Single-headed arrows indicate the hypothesized direction of causation. Red solid lines indicate significantly positive relationships, blue solid lines indicate significantly

negative relationships, red dotted lines indicate non-significantly positive relationships, and blue dotted lines indicate non-significantly negative relationships. **B** Bar graphs are the standardized effects from the SEM on three fluxes. Soil properties represent the first component by the principal component analysis for soil temperature, water content, pH, porosity, dry-sieving mean weight diameter, wet-sieving mean weight diameter, and belowground biomass. Asterisks indicate the statistical significance (***) $p < 0.001$, (**) $p < 0.01$, and (*) $p < 0.05$.

microbial survival³⁷. In contrast, excessive organic matter decomposition may break resource balance through soil acidification and reduce resource availability of microbial communities in the completely thawed period^{38,39}. Also, high nutrient demand by plants during this period may exacerbate the resource competition between microorganisms and plants⁴⁰, both of which can potentially lead to a decrease in microbial diversity. Furthermore, the nutrients were basically frozen and not effectively utilized by microorganisms in the completely frozen period⁴¹. Secondly, microbial activity and richness can be inhibited owing to the sub-zero environment in the completely frozen period⁴². While higher soil water content and soil temperature in the completely thawed period (see Supplementary Notes for details) may suppress the growth of more competitive, cold-adapted, and strict aerobic microorganisms, contributing to decreased diversity⁴³. Conversely, the frequent soil temperature fluctuations during the freeze-thaw stage and in 0–10 cm layer can provide more heterogeneous habitats that are conducive to the survival of microorganisms with various physiological and adaptive capacities^{44,45}. We also observed that diurnal freeze-thaw cycles increased microbial richness, leading credence to our findings of higher diversity during the freeze-thaw stage (Supplementary Fig. S16).

We have validated the hypothesis that microbial communities can maintain higher stability during the freeze-thaw stage compared to the non-freeze-thaw stage. This may be attributed to the broader microbial niche breadth during the freeze-thaw stage (Supplementary Fig. S17), because microorganisms in these periods can utilize a wider range of resources and thereby be more resilient to environmental changes³¹. This is also evidenced by the lower network complexity as represented by multiple network properties³¹, stronger ability to resist disturbances due to greater robustness⁴⁶, and more keystone taxa on account of their important roles in maintaining the network structure during the freeze-thaw stage and in 0–10 cm layer²⁹. Past studies have shown that the fewer microbial interactions can lead to less resource competition, thus reducing the instability caused by resource constraints^{24,47}. Meanwhile, decentralized networks are generally more resilient and resistant because fewer interactions can reduce the risk of propagation if the networks are subjected to external

disturbances^{31,48}. These evidences suggest that fewer bacteria-fungi links and weaker centrality could make microbial communities more stable during the freeze-thaw stage.

Soil gas emissions are one of the key components of soil multifunctionality and can exert largely positive climate feedbacks^{49,50}. We found that CH₄ emission only occurred in the completely frozen period. This is mainly due to the facts that frozen soils can reduce the diffusion of oxygen into the subsurface and facilitate anaerobic conditions in winter, thus inhibiting the microbial methane oxidation process but promoting the methanogenic process⁵¹, where soil temperature played an important role in microbial methanogenic and methane oxidation activities^{52,53}. In contrast, N₂O exhibited a largest uptake in the completely frozen period, which could be attributed to the reduction of N₂O to N₂^{54,55}. It is worth noting that freeze-thaw strength emerged as the most important predictor for N₂O emission, because greater freeze-thaw strength is associated with increased rates of denitrification, which can lead to greater N₂O emission^{56,57}. Past studies have suggested that substrate quality is an important determinant of CO₂ emission and that the exposure and decomposition of soil organic matter can promote carbon mineralization and stimulate soil respiration^{58,59}. As revealed by our study, CO₂ emission was highest in the completely thawed period, when multinutrient exerted an essential contribution. Taken together, both freeze-thaw strength and maximum thawing depth show the positive effects for N₂O and CO₂ fluxes, but a negative effect for CH₄ flux, indicating that increases in freeze-thaw strength will promote N₂O and CO₂ emissions.

We have demonstrated that microbial diversity is positively related to soil multifunctionality, especially during the freeze-thawing stage. These findings align with a previous study suggesting that higher microbial richness can ensure the better performance of soil multifunctionality resulting from the increased taxa supporting the same functions⁶⁰. Additionally, the harsh habitats of alpine permafrost constrain the ability of microorganisms to perform important biogeochemical cycling by limiting life cycles and physiological activities⁴². Some studies have suggested that network complexity can positively drive biodiversity-

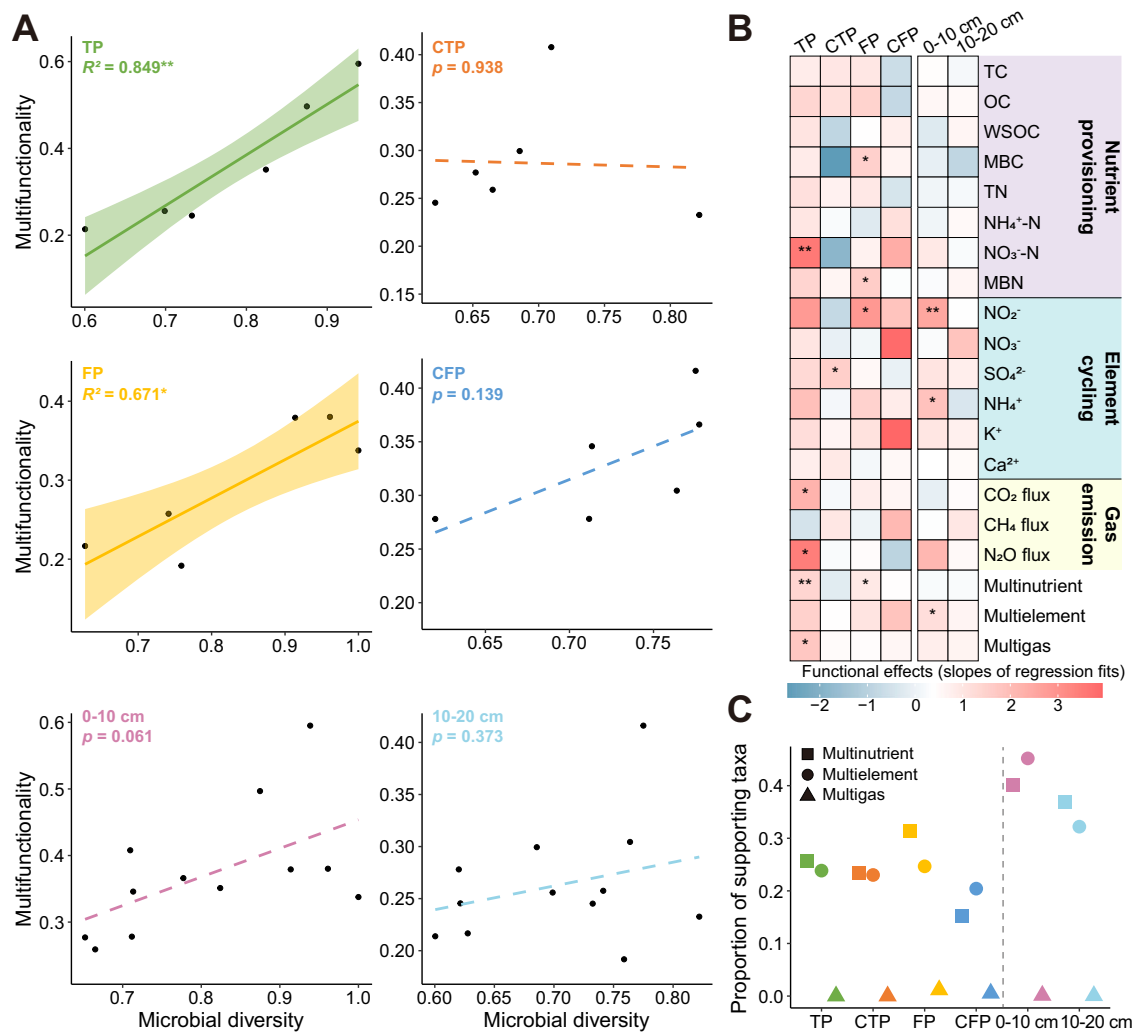


Fig. 3 | Relationships between microbial diversity and soil multifunctionality during four periods of seasonal freeze-thaw processes and at two depths.

A Differences of the linear regression fits between microbial diversity and soil multifunctionality among four periods and at two depths. **B** Differences of functional effects (slopes of regression fits) of microbial diversity on individual functions and classified multifunctionalities among four periods and at two depths. **C** Differences of the proportions of diversity in taxa that supporting classified soil

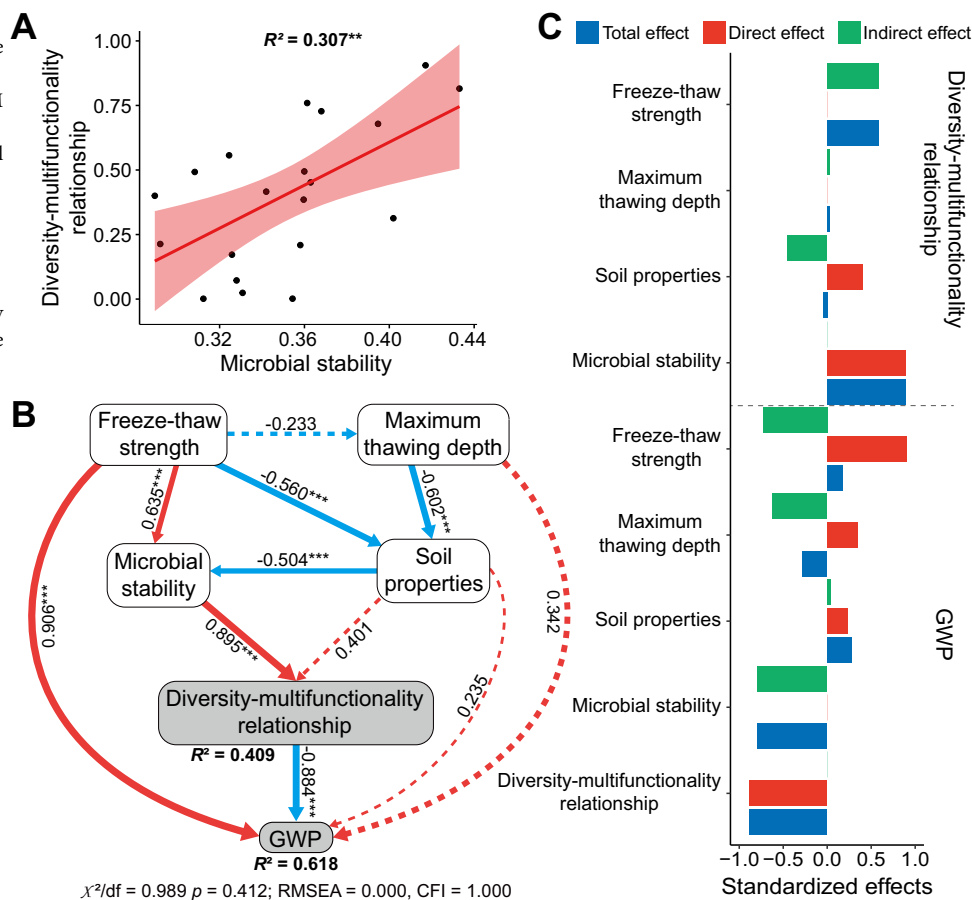
multifunctionalities among four periods and at two depths. Taxa of individual OTUs that are significantly positively correlated with classified multifunctionalities are defined as “supporting taxa”. TC total carbon, OC organic carbon, WSOC water soluble organic carbon, MBC microbial biomass carbon, TN total nitrogen, MBN microbial biomass nitrogen. TP, CTP, FP, and CFP represent the thawing, completely thawed, freezing, and completely frozen periods, respectively. Asterisks indicate the statistical significance (** $p < 0.001$, ** $p < 0.01$, and * $p < 0.05$).

ecosystem multifunctionality or nutrient cycling relationships in agricultural fields and saline urban reservoirs^{21,61}. Given the negative links between stability and network complexity, this actually reflects that these relationships are negatively correlated with microbial stability³¹. Interestingly, we found the opposite result that microbial stability was positively associated with the diversity-soil multifunctionality relationship. Unlike resource-rich agricultural fields, more stable microorganisms may tend to form more efficient and positive interactions to utilize the limited resources and enhance the performance of functions by cooperative work in alpine permafrost^{62–64}. This enables microbial communities to maintain relatively unchanged abilities to perform functions in the face of external shocks^{65,66}. When microbial communities are destabilized, increased competitions within communities may weaken or destroy the performance of certain functions, even cause a negative diversity-soil multifunctionality relationship^{61,67}. To the best of our knowledge, this is one of the first studies to link microbial stability with the diversity-soil multifunctionality relationship, which adds an important dimension to our understandings of this relationship and advances our ability to predict and regulate it. As expected, increasing freeze-thaw strength could promote

the greenhouse effect. Freeze-thaw strength exhibited a driving effect on GWP, while GWP was negatively correlated with the microbial diversity-soil multifunctionality relationship, which is the most intriguing finding. In general, increased freeze-thaw strength due to the changes in freeze-thaw events, especially the extending duration of the freeze-thaw stage under future warming, will promote the intensification of the greenhouse effect, whereas the enhancement of the microbial diversity-soil multifunctionality relationship will alleviate this intensified effect.

In this study, we presented a conceptual paradigm of main content in our study to describe the roles of microbial communities in influencing soil multifunctionality during the four periods of seasonal freeze-thaw processes in the active layer of alpine permafrost (Fig. 5). Briefly, both microbial diversity and stability were higher during the freeze-thaw stage (thawing and freezing periods) than the non-freeze-thaw stage (completely thawed and frozen periods). Microbial diversity maintained positive correlations with soil multifunctionality only during the freeze-thaw stage, and the diversity-soil multifunctionality relationship was driven by the stability of microbial communities. Importantly, greenhouse gas emissions were promoted by increased freeze-thaw strength, which could result in potential positive

Fig. 4 | Linking microbial stability, diversity-soil multifunctionality relationship, and GWP. **A** The linear relationship between microbial stability and diversity-soil multifunctionality relationship. **B** SEM describing the effects of freeze-thaw strength, maximum thawing depth, soil properties, and microbial stability on diversity-soil multifunctionality relationship and GWP. Single-headed arrows indicate the hypothesized direction of causation. Red solid lines indicate significantly positive relationships, blue solid lines indicate significantly negative relationships, red dotted lines indicate non-significantly positive relationships, and blue dotted lines indicate non-significantly negative relationships. The arrow width is proportional to the strength of the relationship. **C** Bar graphs are the standardized effects from the SEM on the microbial diversity-soil multifunctionality relationship and GWP. Soil properties represent the first component by the principal component analysis for soil temperature, water content, pH, porosity, dry sieving-mean weight diameter, wet-sieving mean weight diameter, and belowground biomass. GWP global warming potential. Asterisks indicate the statistical significance (** $p < 0.001$, ** $p < 0.01$, and * $p < 0.05$).



climate feedback. These findings can help in assessing and anticipating the cascading ecological consequences of shifted freeze-thaw patterns on microbial communities and soil multifunctionality in permafrost under climate warming.

Materials and methods

Description of sampling site

An observational field of the alpine meadow ecosystem (ID: SLP3; 98°16'14" E, 38°21'17" N, Alt.: 4014 m) was selected as a sampling site in permafrost regions of the Shule River headwaters on the western part of the Qilian Mountains, northeastern margin of the QTP, China. This 100 m × 100 m observational field was established and protected by a wire fence in the summer of 2010. According to the meteorological monitoring data, the mean annual air temperature and annual precipitation were -3.49 °C and 417 mm, respectively. January was the coldest month with a mean air temperature of -16.57 °C, while August was the warmest month with a mean air temperature of 8.96 °C, with an annual range of 25.53 °C and a daily range of 21.17 °C. Similarly, for the soil temperature at 0–20 cm depth, the annual and daily ranges were 23.16 °C and 18.56 °C, respectively. The vegetation coverage is approximately 42% and the dominant plants consist of *Kobresia pygmaea* and *K. humilis*⁶⁸. Soil type is kastanozems based on the WRB classification (IUSS Working Group WRB 2006)^{69,70}. The permafrost belongs to sub-stable alpine permafrost with an active layer thickness of ~2.3 m⁶⁸ and frequently experiences freeze-thaw processes in the active layer surface.

Sample collection and measurement

We installed three replicates of self-developed pump-style soil gas collectors (Chinese Patent No. ZL201120073304.2) at two soil depths including 0–10 cm and 10–20 cm in July 2011, respectively. In 2013, the in-situ experiments were performed across four periods of

seasonal freeze-thaw processes including the thawing period (28 April and 4 May), the completely thawed period (1 August), the freezing period (29 September and 5 October), and the completely frozen period (31 December) (Supplementary Fig. S1). Each period was represented by the respective sampled time points. Detailed information of the definition and delineation of these periods are provided in the *Statistical Analysis*. Specifically, we selected three squares (50 cm × 50 cm) near the gas collectors for each experiment. After the aboveground vegetation of each square was eliminated, we collected soil samples by combining five soil cores (4.8 cm inner diameter) in an X-shaped pattern from 0–10 cm to 10–20 cm layers, respectively. Notably, soil samples collected twice at 0–10 cm depth during the thawing and freezing periods were mixed and combined into one sample for analysis, respectively. The first sampling times on 28 April and 29 September were considered as the periods before diurnal freeze-thaw cycles. Since diurnal freeze-thaw cycles occurred until the second sampling times on May 4 and October 5, which were defined as the periods after diurnal freeze-thaw cycles. Next, we divided soil samples into three parts. One part was stored in freezer boxes and transported to the laboratory for microbial detection. The second part was stored in cold storage boxes to determine pH, WSOC, NH₄⁺-N, NO₃⁻-N, MBC, and MBN. The last part was air-dried to test the variables including soil specific gravity (SG), major ions (Ca²⁺, K⁺, NH₄⁺, SO₄²⁻, NO₃⁻, and NO₂⁻), OC, total carbon (TC), and total nitrogen (TN). Finally, samples were collected using the above same methods to measure BGB and soil aggregate, respectively. Soil bulk density was measured using a cutting ring (volume of 100 g cm⁻³). Soil temperature and soil water content at two depths were measured using Hydra Probe II soil sensors (Stevens) connected with a CR1000X datalogger (Campbell), which automatically recorded data every ten minutes since July 2011.

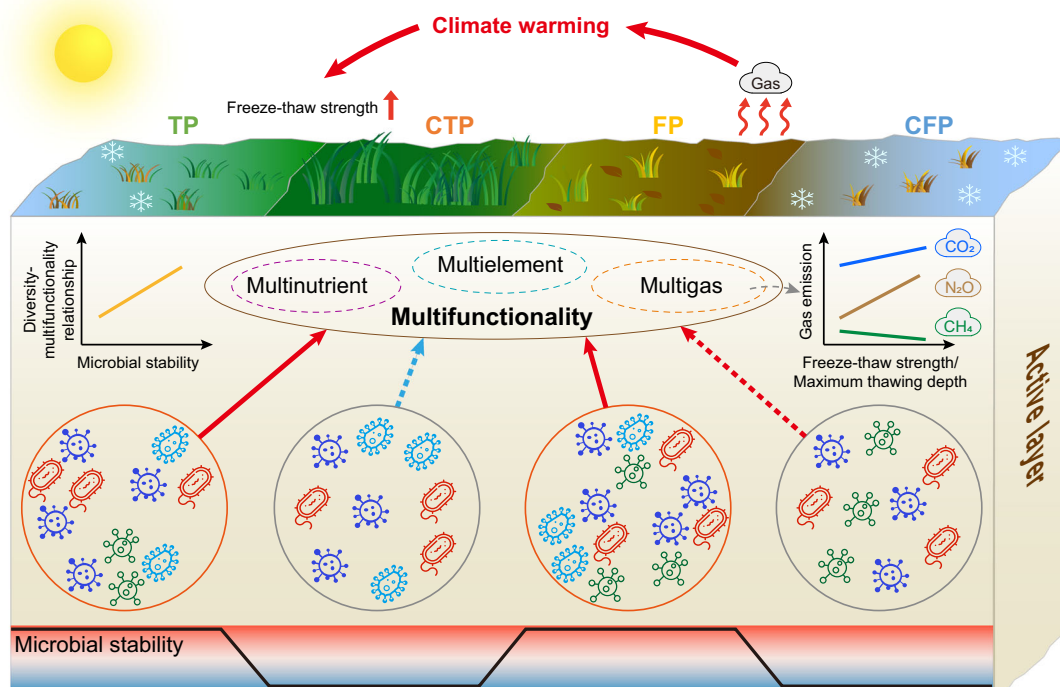


Fig. 5 | Conceptual paradigm of main content in the study showing the role of microbial community in influencing soil multifunctionality during four periods of seasonal freeze-thaw processes in the active layer of alpine permafrost. The orange circles represent the freeze-thaw stage including the thawing and freezing periods, and the grey circles represent the non-freeze-thaw stage including the completely thawed and completely frozen periods. In the circles are different representative microorganisms, more kinds of them mean higher microbial

diversity and more modular arrangements of them mean higher stability. Red solid lines pointing to multifunctionality indicate the significantly positive relationships with diversity, blue dotted line indicates the non-significantly negative relationship, and red dotted line indicates the non-significantly positive relationship. The below color gradient indicates that darker red means higher stability and darker blue means lower stability. TP, CTP, FP, and CFP represent the thawing, completely thawed, freezing, and completely frozen periods, respectively.

Measurements on pH, WSOC, NH₄⁺-N, NO₃⁻-N, MBC, MBN, OC, TC, TN, SG, and Por were described previously^{8,31}. BGB that represents the plant root mass was sampled by soil core (4.8-cm diameter). BGB samples were sieved through a 2-mm mesh following the removal of impurities and then dried at 80 °C until a constant weight was obtained. Dry-sieving mean weight diameter (DMWD) and wet-sieving mean weight diameter (WMWD) that represent the stability of soil aggregate were measured through dry and wet sieving methods, respectively⁷¹. The cations (Ca²⁺, K⁺, and NH₄⁺) and anions (SO₄²⁻, NO₃⁻, and NO₂⁻) were analyzed by DX-600 and ICS-2500 Ion Chromatographs (Dionex), respectively. For soil gas samples, concentrations of CO₂, CH₄ and N₂O were analyzed with 7890A gas chromatography system (Agilent). Their fluxes were calculated based on soil gas concentration gradients based on the previous reference⁷². The frequency and magnitude of soil temperature changes above and below 0.0 °C are generally considered to be the strength of freeze-thaw processes in the active layer, and thus we used the normalized products of frequency (difference between the counts of positive and negative temperatures over a day) and amplitude (sum of absolute values of positive and negative temperatures over a day) of soil temperature change to calculate freeze-thaw strength⁸. Maximum thawing depth is the real-time maximum depth that reflects the soil thawing in permafrost and is consistent with the 0.0 °C-line of soil temperature⁷³. We derived maximum thawing depth using manual boring, soil temperature monitoring, and simulation by the Stefan equation³¹.

Sequencing for microbial communities and bioinformatics

We extracted total DNA from soil samples using the PowerSoil® DNA isolation kit. We then amplified the bacterial 16S rRNA V4-V5 region using the universal primer 515F/806R (515F: GTGCCAGCMGCCGCGGTAA, 907R: CCGTCAATTCMTTTRAGT). The PCR amplified procedure was as

follows: 98 °C for 1 min, followed by 30 cycles of denaturation at 98 °C for 10 s, annealing at 50 °C for 30 s, and elongation at 72 °C for 30 s with final extension at 72 °C for 5 min⁷⁴. Moreover, the ITS1 region of Internal Transcribed Spacer (ITS) gene region of fungi was amplified using universal primer ITS1F/ITS2 (ITS1F: CTTGGTCATTTAGAGGAAGTAA, ITS2: GCTGCG TTCCTTCATCGATGC). All the PCR products were purified by the Agilent 2100 bioanalyzer (Agilent, USA), and then the amplicon libraries were constructed using Illumina TruSeq DNA PCR-Free Library Preparation Kit (Illumina, USA) following the manufacturer's instruction. Due to the different sequence lengths for bacteria and fungi, the validated amplicon libraries were sequenced on the Illumina MiSeq platform using the PE250 bp Paired-end models for bacterial amplicon libraries whereas PE300 bp models for fungal libraries at BGI-Wuhan (Wuhan, China), and more than 50 million base-pairs (Mbp) of raw sequencing reads for each sample were generated.

We adjusted raw data for each sample using QIIME software (Quantitative Insights Into Microbial Ecology, v1.9.1) to remove low-quality sequences, and FLASH software (Fast Length Adjustment of Short reads, v1.2.11) to assemble and merge pairs of sequences into a single high-variance tag sequence using overlap relationships, where singleton sequences without overlap relationships were removed. The tag sequences were then clustered into operational taxonomic units (OTUs) by USEARCH software (Ultra-fast sequence analysis, v7.0.1090) with a 97% threshold to obtain OTU representative sequences. After removing the chimeric sequence, the OTU representative sequences were compared with Greengene_2013_5_99 (v201305) and UNITE (v7.2) databases using RDP classifier software (v2.2) to obtain species annotations with a confidence threshold set to 0.6. The tag sequences were mapped to the OTU representative sequences to obtain OTU and species-annotated abundance tables.

To ensure that subsequent analyses of species diversity were compared with equal sampling, we rarefied data by randomly subsampling 50,000 sequences for bacterial and fungal samples using the minimum number of total sequences in each sample (flattening analysis).

Statistical analysis

Based on the monitoring data of soil temperature across an entire year, the number of completely thawed days, completely frozen days, and freeze-thaw days were calculated as the number of days with the diurnal minimum Ts being $>0.0^{\circ}\text{C}$, the diurnal maximum Ts being $\leq 0.0^{\circ}\text{C}$, and the diurnal maximum Ts being $>0.0^{\circ}\text{C}$ but the diurnal minimum Ts being $\leq 0.0^{\circ}\text{C}$, respectively. We then divided the entire seasonal freeze-thaw processes into four periods (see Supplementary Notes for details): the thawing period, which started from the first day of three consecutive freeze-thaw days in spring; the completely thawed period, which initiated with the first day of three consecutive completely thawed days in summer; the freezing period, which started with the first day of three consecutive freeze-thaw days in autumn; and the completely frozen period, which begun with the first day of three consecutive completely frozen days in winter^{1,8}. Additionally, periods where the freeze-thaw strength equaled to 0 (completely thawed and frozen periods), were combined into the non-freeze-thaw stage. Conversely, periods where the freeze-thaw strength is greater than 0 (thawing and freezing periods) were combined into the freeze-thaw stage.

We performed all statistical analyses in R (V3.5.3; <http://www.r-project.org/>), and created data visualizations using the “ggplot2” package. Richness was selected as a metric of microbial diversity and was calculated via the “vegan” package. Subsequently, we standardized the bacterial and fungal diversity on a scale from 0 to 1, and took the average value as the microbial diversity. Seventeen soil parameters associated with various aspects of a suite of soil functions (multifunctionality) were assessed and distinguished into three categories, including nutrient provisioning (multinutrient), element cycling (multielement), and gas emission (multigas). Specifically, we characterized the functions related to nutrient provisioning by measuring multiple carbon and nitrogen forms, including TC, OC, WSOC, MBC, TN, $\text{NH}_4^+\text{-N}$, $\text{NO}_3^-\text{-N}$, and MBN. The functions related to element cycling was represented by the measurements of multiple anions and cations, including Ca^{2+} , K^+ , NH_4^+ , SO_4^{2-} , NO_3^- , and NO_2^- . Multiple gas fluxes, including CO_2 , CH_4 , and N_2O fluxes, were measured to characterize the functions related to gas emission. These 17 functions were standardized on a scale from 0 to 1 as the individual functions. We used several methods to determine soil multifunctionality including average, weighted, and multi-threshold multifunctionality methods. First, we averaged the standard values of the individual functions to obtain three classified soil multifunctionalities, which were further averaged to obtain soil multifunctionality^{75,76}. Second, we calculated the weighted soil multifunctionality by averaging all individual functions after weighting of TN, TC, and OC with a weight of 1/3 to down-weight highly correlated functions ($R^2 > 0.7$) (Fig. S18), so that these correlated functions had a combined weight of only 1^{77,78}. Average multifunctionality was highly correlated with weighted multifunctionality (Fig. S19A). Third, we calculated the number of functions beyond a given threshold (25%, 50%, 75%, and 90%) and each threshold represents a functional performance level^{20,75}. Importantly, we found basically the same findings about the relationships between microbial diversity and soil multifunctionality using these three methods, suggesting that the choice of multifunctionality index did not alter our results (Figs. 3A, S19B, and S20). Linear regressions were performed between microbial diversity with soil individual functions, classified soil multifunctionalities, and soil multifunctionality. We further employed the linear regressions to define OTUs that were significantly ($p < 0.01$) positively correlated with classified soil multifunctionalities as “supporting taxa”. To examine the ability of each gas to trap heat in the atmosphere relative to CO_2 over a

period of 100 years, we calculated the GWP by the following equation⁷⁹: $\text{GWP} = \text{CO}_2 + \text{N}_2\text{O} \times 273 + \text{CH}_4 \times 27.9$.

SparCC method was used to construct microbial co-occurrence networks³¹. We applied filtering criteria to the SparCC results, retaining only correlations with an $R > 0.8$ and a false discovery rate < 0.05 . Network graphs were generated using the “igraph” package, and network properties were calculated, including nodes, edges, density, average path length, modularity, transitivity, degree, closeness centrality, betweenness centrality, and linkage density (degree/nodes). Network robustness was tested by attacking edges on natural connectivity and the average variation degree was directly used to calculate microbial stability (1 - average variation degree)^{32,80}. Additionally, we extracted the subnetworks of the individual samples and calculated their properties, including degree, average path length, density, transitivity, linkage density, and modularity, to estimate the network complexity using principal coordinate analysis. The sparsity within the networks was indicated by the average path length and modularity, which were calculated as the inverse of the respective variables prior to calculating the complexity. The nodes in each network were classified into different topological roles based on their within-module connectivity (Z_i) and among-module connectivity (P_i) values: module hubs ($Z_i \geq 2.5$, $P_i < 0.62$), network hubs ($Z_i \geq 2.5$, $P_i \geq 0.62$), connectors ($Z_i < 2.5$, $P_i \geq 0.62$) and peripherals ($Z_i < 2.5$, $P_i < 0.62$). Except for peripherals, the other three categories are regarded as keystone taxa due to their crucial roles in stabilizing the network structure²⁹. In summary, we assessed microbial network stability by three methods, including the calculations of network complexity, number of keystone taxa, and robustness. Previous studies have demonstrated that the networks with lower complexity⁴⁶, more keystone taxa²⁹, and stronger robustness³¹ are more stable. Although microbial network stability can reflect the stability of communities^{31,34}, we directly calculated microbial stability by average variation degree³² to validate the results obtained by the network approach.

Random forest models were used to detect variables affecting microbial diversity, stability, soil multifunctionality, and diversity-soil multifunctionality relationship. We applied the moving window approach to explore the determinants of the microbial diversity-soil multifunctionality relationship with the window size of five samples²¹. After the samples were ordered across four periods and two depths, windows were advanced across the samples to generate neighboring subsets to better estimate the linkage between microbial stability and the diversity-soil multifunctionality relationship. The R^2 of the linear regression between microbial diversity and soil multifunctionality was used to characterize the diversity-soil multifunctionality relationship²¹. We further constructed SEM to explore the variables affecting the soil gas fluxes, diversity-soil multifunctionality relationship, and GWP using AMOS 21.0 (Amos Development Corporation). Soil properties represent the first component from the principal component analysis conducted for soil temperature, water content, pH, Por, WMWD, DMWD, and BGB. The goodness of model fit was evaluated based on the χ^2 test ($0 \leq \chi^2/\text{df} \leq 2$ and $0.05 \leq p \leq 1.00$) and the RMSEA ($0 \leq \text{RMSEA} \leq 0.05$ and $0.10 \leq p \leq 1.00$). Generalized linear models were used to assess the relative influence of environmental variables, microbial diversity, stability, multinutrient, and multielement on CO_2 , CH_4 , N_2O fluxes, and multigas with the “h2o” package.

We performed one-way ANOVA to calculate the differences in environmental variables, microbial diversity, microbial network properties, stability, and soil functions among four periods of seasonal freeze-thaw processes at 0–20 cm depth. Student’s t-test was used to calculate their differences between the freeze-thaw stage and the non-freeze-thaw stage at 0–20 cm depth, as well as between 0–10 cm and 10–20 cm layers regardless of periods.

Data availability

The data that support the findings of this study have been deposited in the CNSA of CNGBdb with accession code CNP0001093.

Received: 19 February 2024; Accepted: 4 October 2024;

Published online: 10 October 2024

References

- Chen, S. et al. Soil thermal regime alteration under experimental warming in permafrost regions of the central Tibetan Plateau. *Geoderma* **372**, 114397 (2020).
- Grogan, P., Michelsen, A., Ambus, P. & Jonasson, S. Freeze-thaw regime effects on carbon and nitrogen dynamics in sub-arctic heath tundra mesocosms. *Soil Biol. Biochem.* **36**, 641–654 (2004).
- Li, T. et al. Shortened duration and reduced area of frozen soil in the Northern Hemisphere. *Innovation* **2**, 100146 (2021).
- Ran, Y. et al. Permafrost degradation increases risk and large future costs of infrastructure on the Third Pole. *Commun. Earth Environ.* **3**, 238 (2022).
- Li, X., Jin, R., Pan, X., Zhang, T. & Guo, J. Changes in the near-surface soil freeze-thaw cycle on the Qinghai-Tibetan Plateau. *Int. J. Appl. Earth Obs. Geoinf.* **17**, 33–42 (2012).
- Wang, C., Zhao, W. & Cui, Y. Changes in the seasonally frozen ground over the Eastern Qinghai-Tibet Plateau in the past 60 years. *Front. Earth Sci.* **8**, 270 (2020).
- Chen, T., Jiao, J., Wang, H., Zhao, C. & Lin, H. Progress in research on soil erosion in Qinghai-Tibet Plateau. *Acta Pedol. Sin.* **57**, 547–564 (2020).
- Jia, Y. et al. Improved permafrost stability by revegetation in extremely degraded grassland of the Qinghai-Tibetan Plateau. *Geoderma* **430**, 116350 (2023).
- Rinke, A. et al. Arctic RCM simulations of temperature and precipitation derived indices relevant to future frozen ground conditions. *Glob. Planet. Change* **80–81**, 136–148 (2012).
- Ebrahimi, A. & Or, D. Mechanistic modeling of microbial interactions at pore to profile scale resolve methane emission dynamics from permafrost soil. *J. Geophys. Res. Biogeosci.* **122**, 1216–1238 (2017).
- Oztas, T. & Fayetorbay, F. Effect of freezing and thawing processes on soil aggregate stability. *Catena* **52**, 1–8 (2003).
- Ji, X., Liu, M., Yang, J. & Feng, F. Meta-analysis of the impact of freeze-thaw cycles on soil microbial diversity and C and N dynamics. *Soil Biol. Biochem.* **168**, 108608 (2022).
- Liu, M., Feng, F., Cai, T. & Tang, S. Fungal community diversity dominates soil multifunctionality in freeze-thaw events. *Catena* **214**, 106241 (2022).
- Zhao, Y. & Hu, X. Seasonal freeze-thaw processes regulate and buffer the distribution of microbial communities in soil horizons. *Catena* **231**, 107348 (2023).
- Ren, J. et al. Shifts in soil bacterial and archaeal communities during freeze-thaw cycles in a seasonal frozen marsh, Northeast China. *Sci. Total Environ.* **625**, 782–791 (2018).
- Shi, G. et al. Effects of biochar and freeze-thaw cycles on the bacterial community and multifunctionality in a cold black soil area. *J. Environ. Manag.* **342**, 118302 (2023).
- Hirst, C. et al. Evidence for late winter biogeochemical connectivity in permafrost soils. *Commun. Earth Environ.* **4**, 85 (2023).
- Gao, D., Bai, E., Yang, Y., Zong, S. & Hagedorn, F. A global meta-analysis on freeze-thaw effects on soil carbon and phosphorus cycling. *Soil Biol. Biochem.* **159**, 108283 (2021).
- Hou, R. et al. Effects of biochar and straw on greenhouse gas emission and its response mechanism in seasonally frozen farmland ecosystems. *Catena* **194**, 104735 (2020).
- Delgado-Baquerizo, M. et al. Microbial diversity drives multifunctionality in terrestrial ecosystems. *Nat. Commun.* **7**, 10541 (2016).
- Jiao, S., Lu, Y. & Wei, G. Soil multitrophic network complexity enhances the link between biodiversity and multifunctionality in agricultural systems. *Glob. Change Biol.* **28**, 140–153 (2022).
- Qiu, L. et al. Erosion reduces soil microbial diversity, network complexity and multifunctionality. *ISME J.* **15**, 2474–2489 (2021).
- Hu, W. et al. Aridity-driven shift in biodiversity–soil multifunctionality relationships. *Nat. Commun.* **12**, 5350 (2021).
- Wang, X. et al. Decreased soil multifunctionality is associated with altered microbial network properties under precipitation reduction in a semiarid grassland. *iMeta* **2**, e106 (2023).
- Yang, Y. et al. Geographical, climatic, and soil factors control the altitudinal pattern of rhizosphere microbial diversity and its driving effect on root zone soil multifunctionality in mountain ecosystems. *Sci. Total Environ.* **904**, 166932 (2023).
- Chen, W. et al. Soil microbial network complexity predicts ecosystem function along elevation gradients on the Tibetan Plateau. *Soil Biol. Biochem.* **172**, 108766 (2022).
- Luo, S. et al. Grassland degradation-induced declines in soil fungal community reduce fungal community stability and ecosystem multifunctionality. *Soil Biol. Biochem.* **176**, 108865 (2023).
- Xu, Z. et al. Depth-dependent effects of tree species identity on soil microbial community characteristics and multifunctionality. *Sci. Total Environ.* **878**, 162972 (2023).
- Liu, S. et al. Ecological stability of microbial communities in Lake Donghu regulated by keystone taxa. *Ecol. Indic.* **136**, 108695 (2022).
- Peng, G. & Wu, J. Optimal network topology for structural robustness based on natural connectivity. *Phys. A* **443**, 212–220 (2016).
- Wu, M. et al. Reduced microbial stability in the active layer is associated with carbon loss under alpine permafrost degradation. *Proc. Natl Acad. Sci.* **118**, e2025321118 (2021).
- Xun, W. et al. Specialized metabolic functions of keystone taxa sustain soil microbiome stability. *Microbiome* **9**, 35 (2021).
- Zhao, L. et al. Soil thermal regime in Qinghai-Tibet Plateau and its adjacent regions during 1977–2006. *Adv. Clim. Change Res.* **7**, 307–316 (2011).
- Montesinos-Navarro, A., Hiraldo, F., Tella, J. L. & Blanco, G. Network structure embracing mutualism-antagonism continuums increases community robustness. *Nat. Ecol. Evol.* **1**, 1661–1669 (2017).
- Li, Y. et al. Freeze-thaw cycles increase the mobility of phosphorus fractions based on soil aggregate in restored wetlands. *Catena* **209**, 105846 (2022).
- Leuther, F. & Schlueter, S. Impact of freeze-thaw cycles on soil structure and soil hydraulic properties. *Soil* **7**, 179–191 (2021).
- Gordon, H., Haygarth, P. M. & Bardgett, R. D. Drying and rewetting effects on soil microbial community composition and nutrient leaching. *Soil Biol. Biochem.* **40**, 302–311 (2008).
- Allison, S. D. & Vitousek, P. M. Responses of extracellular enzymes to simple and complex nutrient inputs. *Soil Biol. Biochem.* **37**, 937–944 (2005).
- Wang, X. et al. Globally nitrogen addition alters soil microbial community structure, but has minor effects on soil microbial diversity and richness. *Soil Biol. Biochem.* **179**, 108982 (2023).
- Broadbent, A. A. D. et al. Climate change disrupts the seasonal coupling of plant and soil microbial nutrient cycling in an alpine ecosystem. *Glob. Change Biol.* **30**, e17245 (2024).
- Schuur, E. A. G. et al. The effect of permafrost thaw on old carbon release and net carbon exchange from tundra. *Nature* **459**, 556–559 (2009).
- Jansson, J. K. & Tas, N. The microbial ecology of permafrost. *Nat. Rev. Microbiol.* **12**, 414–425 (2014).
- Fan, D., Kong, W., Wang, F., Yue, L. & Li, X. Fencing decreases microbial diversity but increases abundance in grassland soils on the Tibetan Plateau. *Land Degrad. Dev.* **31**, 2577–2590 (2020).
- Lv, Z., Gu, Y., Chen, S., Chen, J. & Jia, Y. Effects of autumn diurnal freeze-thaw cycles on soil bacteria and greenhouse gases in the permafrost regions. *Front. Microbiol.* **13**, 1056953 (2022).

45. Horner-Devine, M. C., Carney, K. M. & Bohannan, B. J. M. An ecological perspective on bacterial biodiversity. *Proc. R. Soc. B Biol. Sci.* **271**, 113–122 (2004).
46. Fan, K. et al. Soil pH correlates with the co-occurrence and assemblage process of diazotrophic communities in rhizosphere and bulk soils of wheat fields. *Soil Biol. Biochem.* **121**, 185–192 (2018).
47. Bahram, M. et al. Structure and function of the global topsoil microbiome. *Nature* **560**, 233–237 (2018).
48. in 't Zandt, D., Kolarikova, Z., Cajthaml, T. & Munzbergova, Z. Plant community stability is associated with a decoupling of prokaryote and fungal soil networks. *Nat. Commun.* **14**, 3736 (2023).
49. Paustian, K. et al. Climate-smart soils. *Nature* **532**, 49–57 (2016).
50. Luo, J. et al. Organic fertilization drives shifts in microbiome complexity and keystone taxa increase the resistance of microbial mediated functions to biodiversity loss. *Biol. Fertil. Soils* **59**, 441–458 (2023).
51. Knoblauch, C., Beer, C., Liebner, S., Grigoriev, M. N. & Pfeiffer, E. M. Methane production as key to the greenhouse gas budget of thawing permafrost. *Nat. Clim. Change* **8**, 309–312 (2018).
52. Koponen, H. T. & Martikainen, P. J. Soil water content and freezing temperature affect freeze-thaw related N₂O production in organic soil. *Nutr. Cycl. Agroecosyst.* **69**, 213–219 (2004).
53. Zhao, S. et al. Freeze-thaw cycles have more of an effect on greenhouse gas fluxes than soil water content on the eastern edge of the Qinghai-Tibet Plateau. *Sustainability* **15**, 928 (2023).
54. Chapuis-Lardy, L., Wrage, N., Metay, A., Chotte, J. & Bernoux, M. Soils, a sink for N₂O? A review. *Glob. Change Biol.* **13**, 1–17 (2007).
55. Wu, D. et al. N₂O consumption by low-nitrogen soil and its regulation by water and oxygen. *Soil Biol. Biochem.* **60**, 165–172 (2013).
56. King, A. E., Rezanezhad, F. & Wagner-Riddle, C. Evidence for microbial rather than aggregate origin of substrates fueling freeze-thaw induced N₂O emissions. *Soil Biol. Biochem.* **160**, 108352 (2021).
57. Gao, D. & Bai, E. Influencing factors of soil nitrous oxide emission during freeze-thaw cycles. *Chin. J. Plant Ecol.* **45**, 1006–1023 (2021).
58. Yang, S., He, Z. & Chen, L. Different responses of CO₂ and CH₄ to freeze-thaw cycles in an alpine forest ecosystem in northwestern China. *Sci. Total Environ.* **863**, 160886 (2023).
59. Larsen, K. S., Jonasson, S. & Michelsen, A. Repeated freeze-thaw cycles and their effects on biological processes in two arctic ecosystem types. *Appl. Soil Ecol.* **21**, 187–195 (2002).
60. Wagg, C., Schlaeppi, K., Banerjee, S., Kuramae, E. E. & van der Heijden, M. G. A. Fungal-bacterial diversity and microbiome complexity predict ecosystem functioning. *Nat. Commun.* **10**, 4841 (2019).
61. Mo, Y. et al. Microbial network complexity drives non-linear shift in biodiversity-nutrient cycling in a saline urban reservoir. *Sci. Total Environ.* **850**, 158011 (2022).
62. Wagg, C., Bender, S. F., Widmer, F. & van der Heijden, M. G. A. Soil biodiversity and soil community composition determine ecosystem multifunctionality. *Proc. Natl Acad. Sci.* **111**, 5266–5270 (2014).
63. Liu, L. et al. Response of the eukaryotic plankton community to the cyanobacterial biomass cycle over 6 years in two subtropical reservoirs. *ISME J.* **13**, 2196–2208 (2019).
64. Yu, X., Polz, M. F. & Alm, E. J. Interactions in self-assembled microbial communities saturate with diversity. *ISME J.* **13**, 1602–1617 (2019).
65. Meng, F., Hu, A. & Wang, J. Microbial traits shed light on species distributions, assembly processes and ecosystem functions. *Acta Microbiol. Sin.* **60**, 1784–1800 (2020).
66. Garcia-Garcia, N., Tamames, J., Linz, A. M., Pedros-Alio, C. & Puente-Sanchez, F. Microdiversity ensures the maintenance of functional microbial communities under changing environmental conditions. *ISME J.* **13**, 2969–2983 (2019).
67. Maynard, D. S., Crowther, T. W. & Bradford, M. A. Competitive network determines the direction of the diversity-function relationship. *Proc. Natl Acad. Sci.* **114**, 11464–11469 (2017).
68. Chen, S. et al. Response characteristics of vegetation and soil environment to permafrost degradation in the upstream regions of the Shule River Basin. *Environ. Res. Lett.* **7**, 045406 (2012).
69. Liu, W. et al. Storage, patterns, and control of soil organic carbon and nitrogen in the northeastern margin of the Qinghai-Tibetan Plateau. *Environ. Res. Lett.* **7**, 035401 (2012).
70. IUSS Working Group WRB. World reference base for soil resources 2006, 2nd edn. *World Soil Resources Reports No. 103*. FAO, Rome (2006).
71. Zhou, M. et al. Soil aggregates stability and storage of soil organic carbon respond to cropping systems on black soils of Northeast China. *Sci. Rep.* **10**, 265 (2020).
72. Wang, Y. et al. Depth-dependent greenhouse gas production and consumption in an upland cropping system in northern China. *Geoderma* **319**, 100–112 (2018).
73. Li, E. & Dai, J. Determination of the maximum seasonal thawing depth of permafrost in the Northeast. *J. Glaciol. Geocryol.* **3**, 39–43 (1981).
74. Jia, Y. et al. Sequencing introduced false positive rare taxa lead to biased microbial community diversity, assembly, and interaction interpretation in amplicon studies. *Environ. Microbiome* **17**, 43 (2022).
75. Fan, K. et al. Soil biodiversity supports the delivery of multiple ecosystem functions in urban greenspaces. *Nat. Ecol. Evol.* **7**, 113–126 (2023).
76. Lefcheck, J. S. et al. Biodiversity enhances ecosystem multifunctionality across trophic levels and habitats. *Nat. Commun.* **6**, 6936 (2015).
77. Zhang, M. et al. Experimental impacts of grazing on grassland biodiversity and function are explained by aridity. *Nat. Commun.* **14**, 5040 (2023).
78. Manning, P. et al. Redefining ecosystem multifunctionality. *Nat. Ecol. Evol.* **2**, 427–436 (2018).
79. Smith, C. et al. The earth's energy budget, climate feedbacks, and climate sensitivity supplementary material. In *climate change 2021: The physical science basis. Contribution of working group I to the sixth assessment report of the intergovernmental panel on climate change* (2021).
80. Zhang, K. et al. Absolute microbiome profiling highlights the links among microbial stability, soil health, and crop productivity under long-term sod-based rotation. *Biol. Fertil. Soils* **58**, 883–901 (2022).

Acknowledgements

We would like to thank Dr. Jonathan Chase for his assistance with English language and grammatical editing of the manuscript. This work was supported by the National Key Research and Development Program of China (2022YFF1302600), “Light of the West” Cross-team Project of the Chinese Academy of Sciences (xbzg-zdsys-202214), the National Natural Science Foundation of China (41825015, 41871064), and the Science and Technology Program of Gansu Province (23ZDFA017).

Author contributions

All authors contributed intellectual input and assistance to this study and manuscript preparation. S.Y.C. designed research; S.Y.C., J.H.W., and Y.Z.G. performed research; S.Y.C. handled all soil sampling and provided field data; J.W.C. contributed high-throughput sequencing; Y.Z.G., E.Y.L., and M.H.W. performed data analysis and integration with help from R.Q.B. and M.Y.Z.; Y.Z.G. and S.Y.C. wrote the paper with help from A.B., E.Y.L., M.H.W., J.H.W., X.L.C., P.Z.Y., and Q.F.

Competing interests

The authors declare no competing interests.

Additional information

Supplementary information The online version contains supplementary material available at <https://doi.org/10.1038/s43247-024-01765-1>.

Correspondence and requests for materials should be addressed to Shengyun Chen or Jihua Wu.

Peer review information *Communications Earth & Environment* thanks the anonymous reviewers for their contribution to the peer review of this work. Primary Handling Editors: D'Arcy Meyer-Dombard and Joe Aslin. A peer review file is available.

Reprints and permissions information is available at <http://www.nature.com/reprints>

Publisher's note Springer Nature remains neutral with regard to jurisdictional claims in published maps and institutional affiliations.

Open Access This article is licensed under a Creative Commons Attribution-NonCommercial-NoDerivatives 4.0 International License, which permits any non-commercial use, sharing, distribution and reproduction in any medium or format, as long as you give appropriate credit to the original author(s) and the source, provide a link to the Creative Commons licence, and indicate if you modified the licensed material. You do not have permission under this licence to share adapted material derived from this article or parts of it. The images or other third party material in this article are included in the article's Creative Commons licence, unless indicated otherwise in a credit line to the material. If material is not included in the article's Creative Commons licence and your intended use is not permitted by statutory regulation or exceeds the permitted use, you will need to obtain permission directly from the copyright holder. To view a copy of this licence, visit <http://creativecommons.org/licenses/by-nc-nd/4.0/>.

© The Author(s) 2024